

Hamed Ramezani¹, Seyed Naser Azizi^{1,*} and Giancarlo Cravotto²

Improved removal of methylene blue on modified hierarchical zeolite Y: Achieved by a “destructive-constructive” method

<https://doi.org/10.1515/gps-2019-0043>

Received October 31, 2018; accepted May 16, 2019.

Abstract: In this study removal of methylene blue (MB) from an aqueous solution by zeolite (NaY) and related modified hierarchical zeolite (MY) has been investigated. The NaY zeolite with a low ratio of Si/Al was synthesized from silica extracted rice husk ash. It was transformed to hierarchical zeolite (MY) by a “destructive-constructive” modification method using tetramethyl ammonium hydroxide (TMAOH) and a cationic surfactant (Cetyltrimethylammonium bromide, CTAB) as a templating agent. Various characterization method like FT-IR, XRF, XRD, BET, TGA, SEM and BJH confirmed the construction of parent zeolite and also successfulness of the modification process. EDX showed a negligible change of Si/Al ratio during modification which is favorite in adsorption of cationic MB dye. In order to study the interaction between the surface of adsorbent and adsorbate, six common isotherms were used. By Langmuir isotherm, it is clarified that, the maximum adsorption capacity (q_m) had improvement from 15.2 mg g⁻¹ to 133.1 mg g⁻¹ for NaY and MY, respectively. The kinetic studies showed that the adsorption obeys the Pseudo-second order model for both NaY and MY zeolites. Also, the usage frequency of the MY was investigated. Results showed that there was not any noticeable change in performance of adsorption after four circles.

Keywords: zeolite NaY; hierarchical zeolite; methylene blue; destructive-constructive method; adsorption

* **Corresponding author: Seyed Naser Azizi**, Analytical Division, Faculty of Chemistry, University of Mazandaran, 47416-95447 Babolsar, Iran, Tel.: +981135342350, Fax: +981135342380, e-mail: azizi@umz.ac.ir

Hamed Ramezani, Analytical Division, Faculty of Chemistry, University of Mazandaran, 47416-95447 Babolsar, Iran

Giancarlo Cravotto, Dipartimento di Scienza e Tecnologia del Farmaco, University of Turin, Via P. Giuria 9, I-10125 Turin, Italy

1 Introduction

Development of urbanization and industrialization lead to the release of high amounts of wastes into the environment. In addition, drought is spreading in the most area of the world. Therefore wastewater treatment can be a vital issue that nowadays humanity encounter [1]. The presence of dyes in water, even in less than 1 ppm, are strongly observable and also undesirable. They prevent penetration of sunlight into the water, resulting annihilating the aquatic biota health problems such as mutagenic and carcinogenic effects [2,3]. Furthermore, by reducing the oxygen levels in water, suffocation of aquatic flora will happen [2-4]. Methylene blue (MB) belongs to basic dyes which are water-soluble cationic dyes that are mainly applied for dyeing acrylic fibers, wool, silk and cotton [4]. Adsorption is an effective method for water treatment and has a high potential for the removal and recovery of dyes from wastewater. Initial cost, the simplicity of design and ease of operation made it a premier method for purification of water [4]. The most common adsorbent for these purposes is activated carbon [3-5]. However, it suffers from the high cost of production. Also, its regeneration is an inconvenient process [5,6].

Zeolites are aluminosilicates porous materials with a three-dimensional framework. It consists of SiO₄ and AlO₄ tetrahedra as the primary units, which oxygen atom connects these two units [7]. The presence of Al species in the framework of zeolites induce negative charges that compensate by extra framework cations like Na⁺ which is mobile and easily exchangeable by other cations. Based on the number of tetrahedra, there are different pores with different sizes: 8 tetrahedra with small pore size of 0.30-0.45 nm (e.g., zeolite A), 10 tetrahedra with medium pore size of 0.45-0.60 nm (e.g., ZSM - 5), 12 tetrahedra with large pore size of 0.6-0.8 nm (e.g., zeolites Y) and more than 14 tetrahedra extra-large pores (e.g., UTD - 1). These size dependence channels allow capture of molecules in different sizes. In addition, the geometry and morphology of the zeolites channels allow shape-selective adsorption and catalysis on zeolites [6]. The adsorption properties of the zeolites are controllable and depend on Si/Al ratio,

they vary from hydrophobic to hydrophilic type materials [8]. By increasing the Si/Al ratio, the hydrophilicity of zeolite will decrease. The low silica zeolites are aluminum saturated and possess the higher cations concentrations to compensate negative charge induced by inserting the Al in the frameworks. Therefore, they give optimum adsorption properties towards cations and organic molecules with hydrophilic nature [9].

Porous materials based on their pore diameter (d) put into three categories: microporous, $d < 2.0$ nm; mesoporous, $d = 2.0$ -50 nm; macroporous, $d > 50$ nm [8]. There are lots of molecules with the size higher than zeolite pores. It has been proven that the introduction of mesopores within microporous zeolite structures facilitate mass transfer to active sites in zeolites [10,11]. The presence of only micropores in the structure of zeolite cause mass transfer limitations. Pore engineering is a way to improve the accessibility of the zeolites pores. As mentioned before, insertion pores with sizes in the range of mesopores in the presence of micropores in the zeolites which is referred to hierarchical zeolites, could enhance the diffusion path length several order of magnitude faster than in the presence of micropores solely. The creation of mesopores in zeolite crystals is equivalent to increasing the external surface area of the zeolite, result in easier diffusion of larger molecules in zeolite [8,12].

Generally, there are two main strategies in the synthesis of hierarchical zeolites: direct synthesis and post-synthesis; also named as “bottom-up” and “top-down” approaches, respectively [13]. Direct synthesis is a constructive method in which the mesoporosity will be formed along with synthesizing the zeolite by employing soft or hard templates [13]. The usual methods for post-synthesis consist of desilication, dealumination, high temperature steaming and acid leaching. All of these destructive methods are based on creating a defect in the structure of parent zeolite. The mesoporosity will form accidentally and therefore arbitrary mesoporous forms which mainly have located in internal cavities and are inaccessible [10]. Wang et al. and Ying and Garcia-Martinez were the first researchers who utilized the recrystallization of the zeolites in basic media and in the presence of a surfactant as a mesopore directing agent [14,15]. This method which is referred to “destructive-constructive” approach is based on partial demolition and dissolution of the parent zeolite structure by a base like NaOH, TMAOH, Na_2CO_3 , NH_4OH , etc. and then recrystallization of them in the presence of a cationic surfactant (usually CTAB) as a mesoporous template. This method allowed inserting tailored mesopores simultaneously original micropores in zeolites structures rather than uncontrollable and random

non-optimized mesoporosity in other post-synthesis methods.

Zeolite NaY belongs to the faujasite family of zeolites. Its high surface area and relatively large pores, (0.74 nm), low cost, excellent thermal and hydrothermal stability made it a versatile compound in adsorption and catalysis [9]. Despite its exemplary characteristics, zeolite NaY, because of microporous character, like other zeolites, suffer from diffusion problems for bulky molecules. As mentioned above inserting a secondary mesopore (2-50 nm) in addition to the micropores will resolve this deficiency. In this work the zeolite NaY was synthesized by the low cost silica extracted rice husk ash as the silica source. The prepared zeolite carried out the low ratio of Si/Al and therefore had hydrophilic features in comparison with available commercial one, so it was proper for removal of cationic dyes like methylene blue. In order to improve the adsorption process of the bulky methylene blue molecule (1.42×0.611 nm), the presence of micropores (~1.4 nm) solely were not satisfying therefore with a “destructive-constructive” method, as-synthesized zeolite was modified and hierarchical zeolite (MY) was achieved which possessed higher external surface area. The results showed that this hierarchical zeolite MY had improved adsorption capacity in the removal of methylene blue in comparison with parent NaY zeolite.

2 Experimental

2.1 Material and instruments

Hydrochloric acid (37%), sodium hydroxide (98%) and methylene blue were all purchased from Merck. Sodium aluminate was supplied from VWR. Amorphous silica which is one of the raw materials in the synthesis of zeolite NaY, was extracted from rice husk ash and its composition was determined by XRF (about 84% (w/w)). TMAOH 20% and CTAB were prepared from Sigma-Aldrich.

2.2 Apparatus

The elemental composition of the extracted silica was determined by X-ray fluorescence spectrometry (XRF, PHILIPS, model PW 1480). In order to confirm the structure and crystallinity of as-prepared zeolite, an advance Bruker D8 XRD using Cu $K\alpha$ radiation ($\lambda = 0.15406$ nm) was used. The Low angle XRD pattern was achieved by a Panalytical model X'Pert PRO MPD, Netherlands. The

FT-IR spectrum of zeolite was recorded by Bruker Vector 22, Germany. In order to determination of the surface area and porosity, a BET (Quantachrom Nova series) was also used. Thermogravimetric analyzer from Perkin Elmer model TGA 4000 was used for recording the TGA thermogram. The UV-vis spectrophotometer which was utilized for determination of the concentration of MB after adsorption was from Pg instruments, model T90, and an 827 model of Metrohm pH meter was used for measuring the pH of the initial adsorption solution. For investigation of the reusability performance of adsorbent a microwave furnace (Microsynth MILESTONE) has been utilized to calcinate the methylene blue adsorbed onto surface of zeolite.

2.3 Synthesis of hierarchical zeolite from silica extracted rice husk ash

At the first step, the silica was extracted from rice husk ash according to Kalapathy method [16]. The analysis of the extracted powder by XRF showed 84.25% SiO₂ was achieved. Then this value was used for the synthesis of zeolite NaY based on a two-steps seeding technique [7]. Briefly, two types of gels named as seed gel and feed stuck gel were prepared according to molar ratios of 10.67 Na₂O : Al₂O₃ : 10 SiO₂ : 180 H₂O and 4.30 Na₂O : Al₂O₃ : 10 SiO₂ : 180 H₂O, respectively. The seed gel was aged for 24 h and then slowly added to feed stuck gel which prepared and used immediately without aging. The final gel possessed 5% (mol) of the seed gel, resulted in overall gel with a molar ratio of 4.62 Na₂O : Al₂O₃ : 10 SiO₂ : 180 H₂O. This overall gel also was aged for 24 h and then transferred into a Teflon-lined stainless steel autoclave and was crystallized at 90°C for 24 h in order to achieve the crystalline zeolite NaY. Converting the NaY zeolite based on “destructive-constructive” method was according to a procedure that was used by Chal and García-Martínez [17,18]. At first step in order to reach the zeolite HY from zeolite NaY, 1.0 g of parent zeolite was stirred in 1 M ammonium chloride solution at 80°C for 4 h and then washed three times with double distilled water to remove chloride ion. Then the resulted NH₄Y zeolite was calcinated in a muffle furnace for 5 h. The achieved HY was dispersed and stirred for 30 min in 30 mL 0.09 M tetramethyl ammonium hydroxide (TMAOH 25% in water) and 0.5 g hexadecyltrimethylammonium bromide (CTAB). The aforementioned solution was transferred to a Teflon-lined stainless steel autoclave and put in an oven at 150°C for 20 h. Finally, the product was washed with double distilled water and dried overnight at 80°C. Eventually the organic components were eliminated by calcination at 550°C for 8 h.

2.4 Adsorption experiments

2.4.1 Isotherm study

In order to study of the adsorption isotherm, 10 mL of MB solutions with concentrations in the range of 10-100 ppm for NaY and 10-350 ppm for MY were shaken in the presence of 0.02 g of each adsorbents for 1 h. After centrifuge, the residual dye concentrations were determined by spectrophotometer at 664 nm and using a standard calibration curve. In order to calculate the adsorption capacity (q_e), the following equation was utilized:

$$q_e = \frac{(C_0 - C_e)}{m} \times V \quad (1)$$

where C_0 and C_e are the initial and equilibrium concentrations of solutions (mg/L), respectively and m (g) is the amount of adsorbent, V (L) is the volume of the solution. Therefore the adsorption capacity (q_e) was achieved in mg/g.

Then q_e versus C_e was plotted and assessed by various isotherm equations inserted in Table 1. An Origin 8.6 software was used for nonlinear curve fitting by exploiting these equations.

2.4.2 Kinetic study

In order to determine the kinetic parameters of the adsorption process, 0.01 g of NaY and 0.01 g of MY were added to 25 mL of 10 and 20 ppm solutions of MB, respectively. Each solution was stirred in different time intervals until 180 min. Then the adsorption capacity vs. time was plotted. Two kinetic models, Pseudo first order or Lagergren and Pseudo-second order were used in order to evaluate the kinetic. The equation for Pseudo first order model is as follow:

$$q_t = q_e \left(1 - \exp(-k_1 t)\right) \quad (2)$$

where q_t and q_e are the adsorption capacity at time t and in equilibrium, k_1 is the adsorption rate constant. The Pseudo second order can be illustrated as Eq. 3:

$$q_t = \frac{k_2 t q_e^2}{1 + k_2 q_e t} \quad (3)$$

where q_t and q_e are the same as Pseudo- first order parameters and k_2 is the rate constant of pseudo- second order. In order to curve fitting purposes, the Origin software was used.

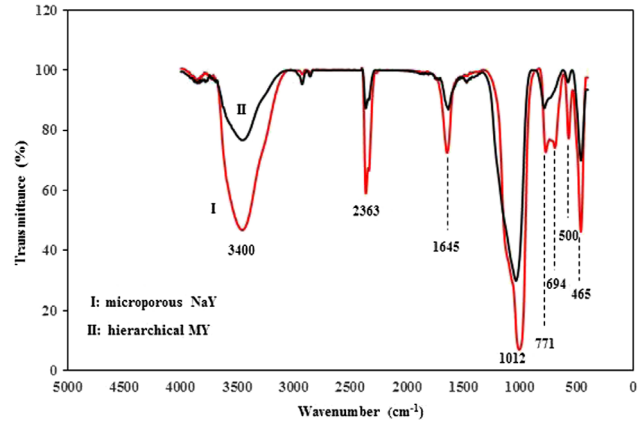
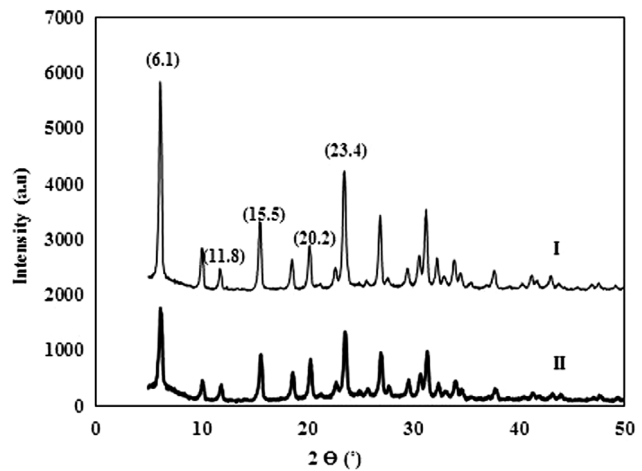
Table 1: Non-linear models of adsorption isotherms and their parameter.

Isotherm	Formula	Parameter
Langmuir	$q_e = \frac{q_m k_L C_e}{1 + k_L C_e}$	q_e : amount of MB adsorbed onto per unit mass of zeolite (mg g^{-1}) q_m : the monolayer or maximum adsorption capacity (mg g^{-1}) C_e : the equilibrium concentration (mg L^{-1}) k_L : affinity of the binding sites and energy of adsorption (l mg^{-1})
Freundlich	$q_e = k_F C_e^{1/n}$	q_e : amount of MB adsorbed at equilibrium (mg g^{-1}) C_e : the equilibrium concentration (mg L^{-1}) k_F , related to the adsorption capacity n : related to adsorption intensity of the sorbent
Redlich-Peterson	$q_e = \frac{AC_e}{1 + BC_e^g}$	q_e : amount of MB adsorbed at equilibrium (mg g^{-1}) C_e : the equilibrium concentration (mg L^{-1}) A , B and g are the Redlich–Peterson parameters
Temkin	$q_e = A + B \ln C_e$	q_e : amount of MB adsorbed at equilibrium (mg g^{-1}) C_e : the equilibrium concentration (mg L^{-1}) A , B and g are the Temkin parameters
Koble-Corrigan	$q_e = \frac{AC_e^n}{1 + BC_e^n}$	q_e : amount of MB adsorbed at equilibrium (mg g^{-1}) C_e : the equilibrium concentration (mg L^{-1}) A , B and n are the Koble–Corrigan parameters
Toth	$q_e = \frac{k_T C_e}{(a_T + C_e)^{1/t}}$	q_e : the adsorbed amount at equilibrium (mg g^{-1}) C_e : the adsorbate equilibrium concentration (mg L^{-1}) a_t : Toth isotherm constant (L/mg) t : Toth isotherm constant k_T : Toth isotherm constant (mg/g)

3 Results and discussion

3.1 Characterization of adsorbents

Figure 1 shows the FT-IR spectra of the microporous NaY and hierarchical MY. There are two categories of characteristic vibration patterns for zeolite NaY which are related to internal and external tetrahedra. The internal tetrahedra included asymmetric and symmetric stretching modes in $1250\text{-}920\text{ cm}^{-1}$ and $720\text{-}650\text{ cm}^{-1}$ and T-O (T=Si or Al) bending vibration at $500\text{-}420\text{ cm}^{-1}$. The vibration

**Figure 1:** FT-IR spectra of (I) microporous NaY and (II) hierarchical MY.**Figure 2:** Wide angle XRD patterns of (I) microporous NaY and (II) hierarchical MY.

related to external linkages consist of asymmetrical and symmetrical stretching modes at $1150\text{-}1050\text{ cm}^{-1}$ and $820\text{-}750\text{ cm}^{-1}$ and double ring vibration at $650\text{-}500\text{ cm}^{-1}$. The above mentioned vibration pattern are assigned in Figure 1. It is seen, after inserting the mesopores, approximately all vibration pattern of zeolite NaY has maintained and only the peak at 694 cm^{-1} has changed which is related to internal tetrahedra symmetric stretching modes and therefore a confirmation of the structure alteration of the zeolite crystals. Broad band at around 3400 cm^{-1} is assigned to OH vibration of adsorbed H_2O . The decrease of its intensity in hierarchical MY is observed which is related to desorption of the proposed water in calcination step during the preparation of hierarchical MY (Section 2.3).

In Figure 2 the wide angle diffractogram could be seen for both parent microporous NaY and hierarchical MY. As can be observed the characteristic peaks at 2θ 6.1° , 11.8° , 15.5° , 20.2° and 23.4° related to a NaY zeolite has maintained after modification to hierarchical MY but

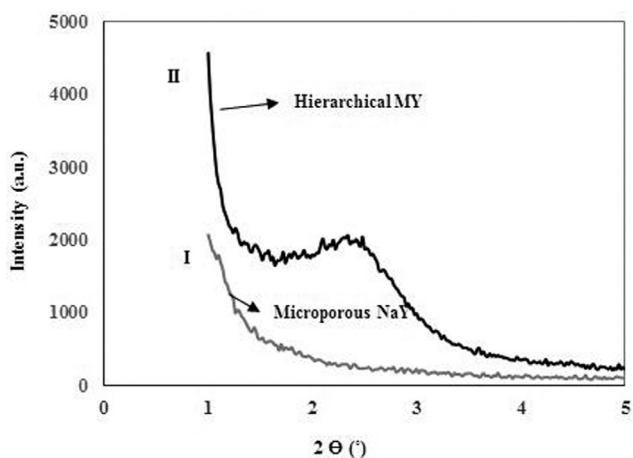


Figure 3: Low angle XRD pattern for (I) microporous NaY and (II) hierarchical MY.

because of partially destructions of parent microporous NaY crystals, which are in charge of the zeolite XRD patterns, and formation of mesoporosity, the intensities of hierarchical MY peaks have been diminished [7,19].

The low angle XRD of the both zeolites has been inserted in Figure 3. It is seen that there is no peak at 2θ of 0.8-5 for parent NaY. In the case of hierarchical MY adsorbent, a peak at 2θ around 2.4° can be seen which implies that the ordered mesoporous pores has been constructed and confirm the successfulness of the “destructive-constructive” modification method in formation of ordered and tailored mesopores. This phenomenon is observed when the template is used to construct of the ordered mesopores [17].

Investigation of the N_2 adsorption-desorption isotherms of the proposed adsorbents is a reliable method

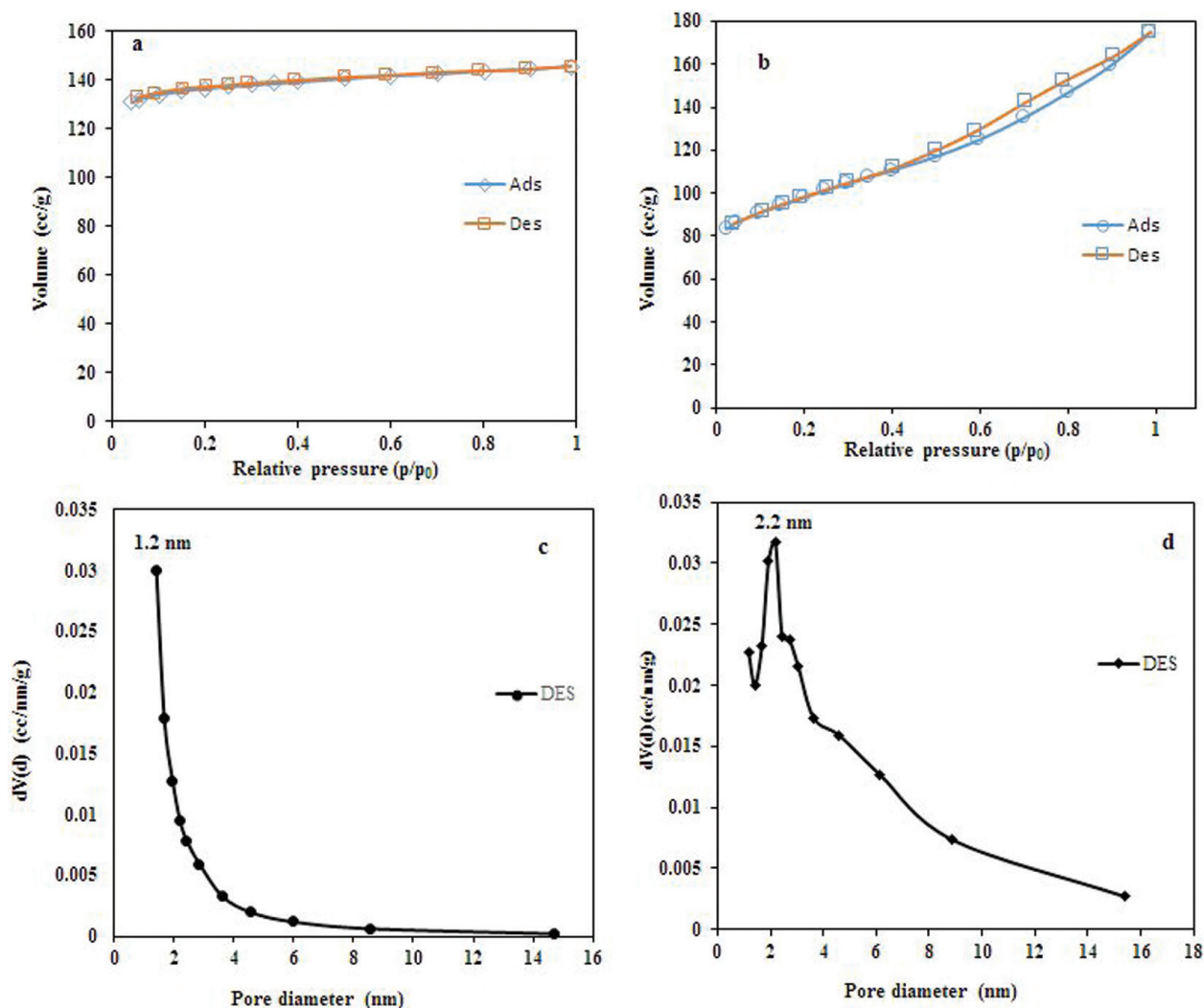


Figure 4: N_2 adsorption-desorption isotherm plots of (a) microporous NaY (b) hierarchical MY and pore size distribution of the (c) microporous NaY, (d) hierarchical MY.

in discriminations between micro and mesopores systems. In Figures 4a and 4b, the isotherms of both parent and modified hierarchical zeolites have been inserted. The horizontal plateau until high relative pressure without any hysteresis is related to a type I isotherm which is the intrinsic characteristic of the materials with the only micropores (Figure 4a) [20]. After modification of as-synthesized zeolite and inserting some typical mesopores, the horizontal plateau with the upward procedure at higher relative pressure could be seen (Figure 4b). This positive slope, instead of the only horizontal saturation plateau along the whole region of isotherm, implies the significant presence of mesoporosity [20]. This order which is a combination of Isotherms I and IV is indicative of a bimodal micropores and mesopores systems [21]. Appearing the hysteresis loop in the isotherm also confirms the presence of mesopores. The horizontal hysteresis loop which is observed in the Figure 4 b could be related to the formation of ink bottle type mesopores. From the t-plot method, the internal surface area was determined and therefore by considering the total surface area achieved by BET method it was clarified that, the external surface area of 32.823 m²/g for microporous NaY has changed to 137.730 m²/g for hierarchical MY. This remarkable growth in external surface area also confirms the formation of the mesopores in the microporous zeolite crystals [12].

Pore size distribution profiles of the NaY and MY are observed in Figures 4c and 4d. By the BJH method and using desorption branch of the nitrogen isotherm, the pore size distribution and the adsorbed volume was calculated. The pore size in the range of only 1.2 nm for microporous NaY could be seen in Figure 4c. In Figure 4d, the BJH of hierarchical MY zeolite is depicted. The presence of a variety of pore size distributions is the manifest of the hierarchical zeolites. As can be seen, there are pore size in the ranges of 1.2 to 6 nm in which the pores size of 2.2 nm are in maximum abundance. The procedure observed in the BJH method is completely in agreement with the data achieved by the BET methods. In Table 2 the textural properties of both microporous NaY and hierarchical MY is inserted.

In Figure 5 the SEM and EDX results of the zeolites has been depicted. The SEM micrograph shows that the synthesized zeolites NaY has well-shaped crystals (Figure 5a). In Figure 5b, which is related to hierarchical MY, it is obvious that, after the modification process no alteration in crystal shape and habit has happened. The EDX analysis of microporous NaY and hierarchical MY (Figures 5c and 5d) corroborates the values of Si/Al ratio for both zeolites are the same and is nearly 2. These results show that during conversion of microporous NaY to hierarchical MY by the proposed “destructive-

Table 2: Surface area and pore volume properties of microporous NaY and related hierarchical MY.

Adsorbents	Total surface area (m ² g ⁻¹) ¹	External surface area (m ² g ⁻¹)	Internal surface area (m ² g ⁻¹)	Internal pore volume (ccg ⁻¹) ²	Average pore diameter (nm) ³
NaY zeolite	458.5	32.823	425.6	0.197	1.4
Hierarchical MY	337.7	137.730	200.0	0.093	2.2

¹ multipoint BET

² t-method

³ calculated from desorption branch of the related isotherm using BJH method

constructive” method, no significant change in Si/Al ratio and therefore no leakage of Al or Si has occurred; hence the hydrophilicity of the original zeolite has maintained which is favorite in adsorption of cationic methylene blue dye.

The thermogravimetric analysis (TGA) of the NaY and MY (Figure 6) show a weight loss at around 100°C which is related to losing the adsorbed water. As can be seen both parent and modified zeolite are stable until high temperatures. As the recovery process of the adsorbents will be performed in high temperature (e.g. 500°C), therefore the stability of them in high temperature is favorite.

In Figure 7, the FT-IR spectra of each adsorbent before and after adsorption of MB on their surfaces has been depicted. As can be seen no noticeable alteration is observed. The lack of any shift in the vibration pattern shows that, there are no chemical bonds between the MB and the atoms in the surface of the both adsorbents. As the zeolite framework possesses strong anionic nature [22] and by considering the cationic charge of MB, therefore it can be concluded that, the electrostatic force is in charge of the adsorption process.

3.2 Adsorption studies

3.2.1 The effect of pH on methylene blue adsorption

In Figure 8 the effect of pH of the initial solution on adsorption process has been studied in the range of 2-12 for both microporous NaY and hierarchical MY zeolites. The pH based adsorption profile for both of them is almost the same. In more acidic and basic pH, the adsorption capacity is low and between about pH 3-10, the optimum adsorption could be observed. This adsorption behavior is similar to other adsorption processes which already observed [23,24]. The lower adsorption capacity at pH below 3 can be related to

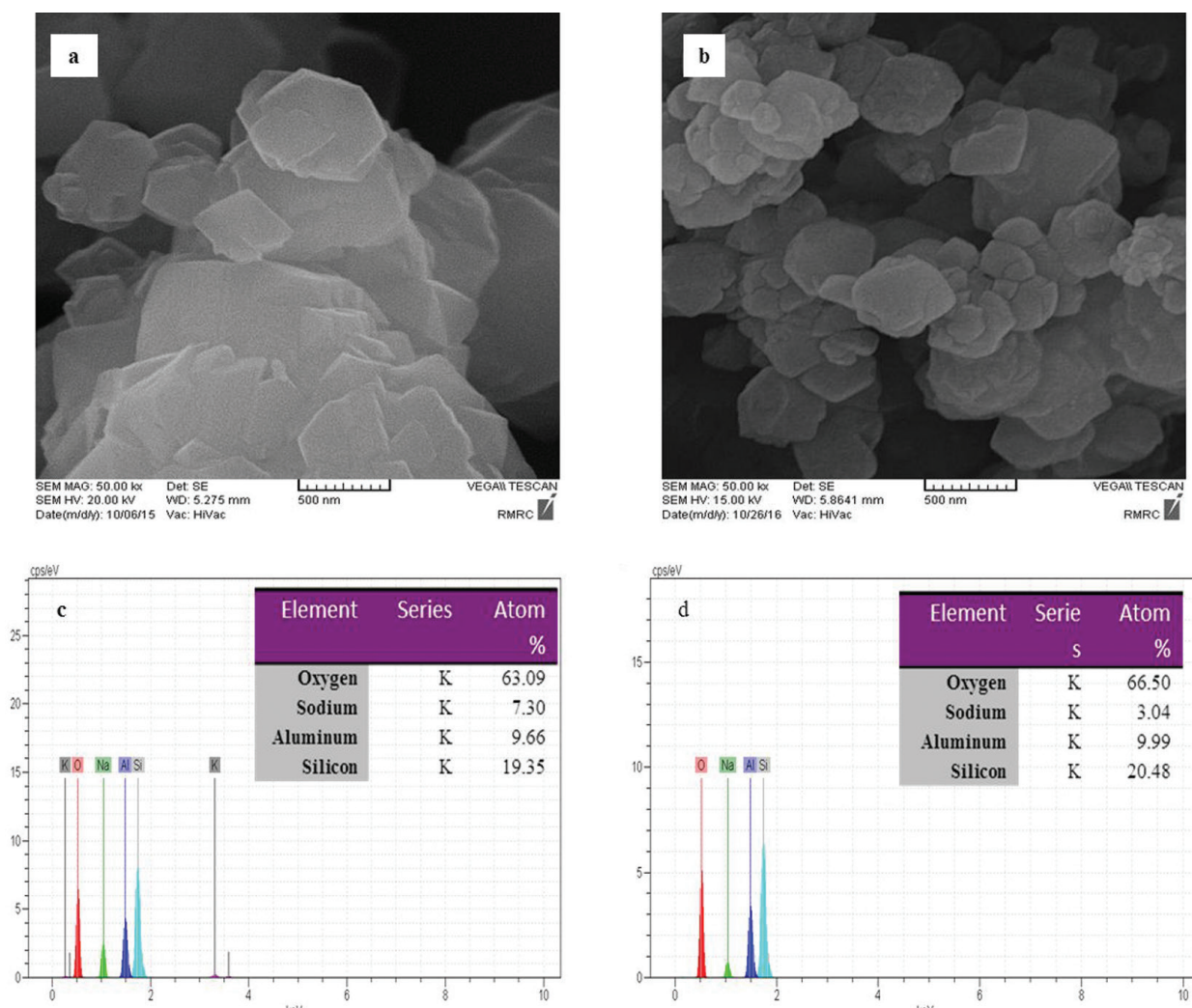


Figure 5: The SEM micrographs of (a) microporous zeolite NaY, (b) hierarchical MY and the EDX plots of (c) microporous NaY, (d) hierarchical MY zeolites; insets show the elemental percentages.

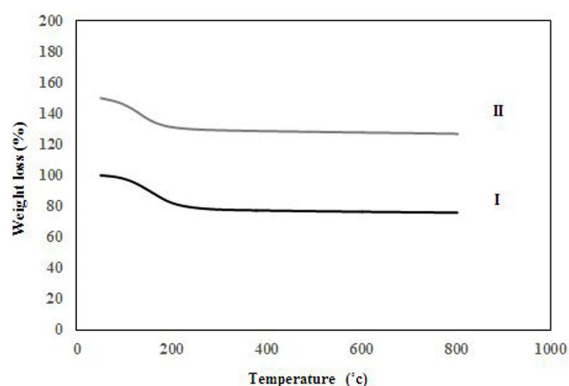


Figure 6: Thermogravimetric analysis (TGA) curve of (I) microporous NaY and (II) hierarchical MY.

the competition between H^+ ions with cationic MB dye on occupying the adsorption sites of zeolites. In our opinion, the decrease in adsorption at higher pH

(more than 11) can be related to the presence of higher amounts of OH^- ions which can compete with the zeolite anionic surface as the adsorption sites.

3.2.2 Adsorption equilibrium studies

In order to better investigation of the adsorption process, it is essential to study the equilibrium. An adsorption equilibrium usually named adsorption isotherm. It shows how an adsorbate interacts with adsorbent surface and also the amount of tendency of adsorbate to adsorbent will be understood [25]. It can also be used to find the maximum adsorption capacity (q_m) of adsorbent. By plotting the solid-phase concentration versus liquid-phase concentration at equilibrium, the adsorption isotherm is achieved whereby certain constants will be attained, containing various information about

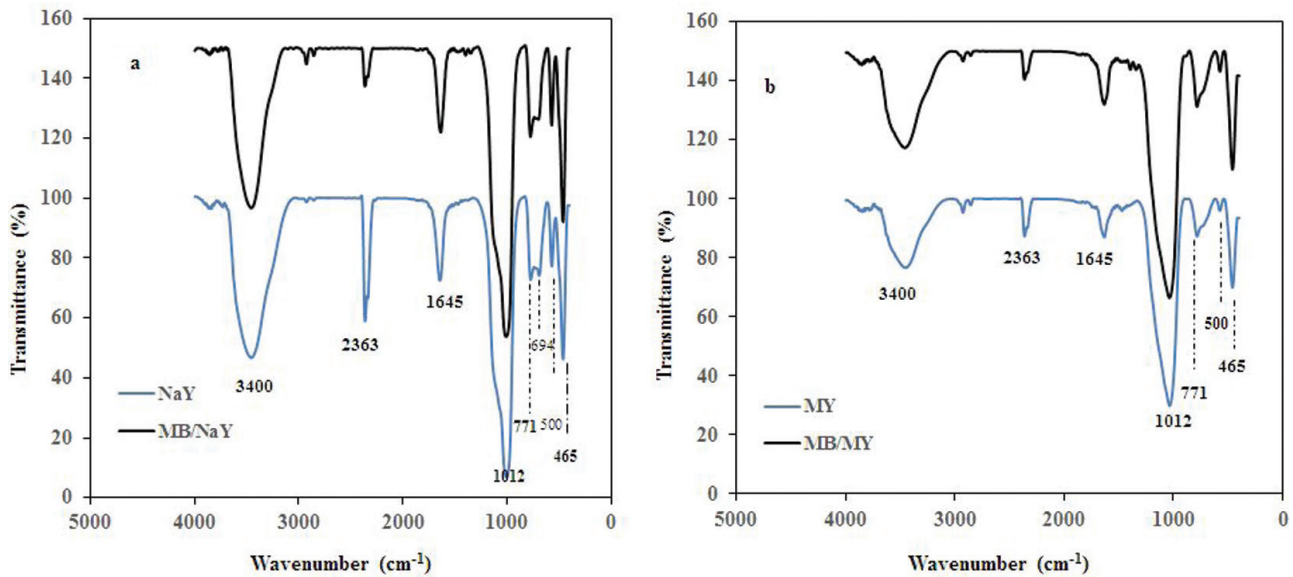


Figure 7: FT-IR spectra of (a) microporous NaY before and after adsorption of methylene blue (MB/NaY) and (b) related FT-IR spectra of hierarchical MY and after adsorption of methylene blue (MB/MY).

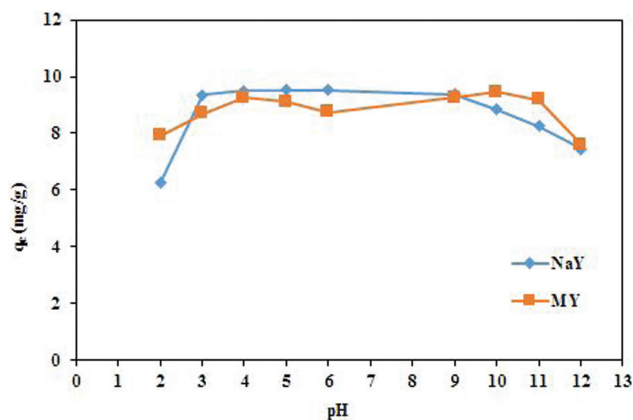


Figure 8: Effect of pH on equilibrium uptake of MB ($m = 0.01$ g, $V = 0.01$ L, $C_0 = 10$ mg/L, $T = 20^\circ\text{C}$, stirring rate = 250 rpm).

the surface properties and affinity of adsorbate to the adsorbent [26]. In order to a comprehensive investigation of the adsorption process, six isotherms (Table 1) has been applied. Figures 9a and 9b show the plots of the related isotherms for MB removal for both adsorbents. Parameters achieved by each isotherm has been inserted in Table 3.

As can be seen, the Langmuir, Redlich-Peterson, Toth, and Temkin possess high correlation coefficient which implies that the adsorption parameters are well matched with the experimental results. The rest isotherms i.e. Freundlich, and Koble-Corrigan also have lower, but acceptable coefficient of determination (R^2). From the Langmuir isotherm, the maximum adsorption capacity (q_m) for parent microporous NaY is calculated to be

15.2 mg/g which was improved to a remarkable amount of 133.1 mg/g for hierarchical MY.

In Table 4, the values of maximum adsorption capacity (q_m) in the removal of MB for various adsorbents has been inserted. As can be seen the q_m for the hierarchical MY has a noticeable amount in comparison with other adsorbents.

The essential characteristics of the Langmuir isotherm is expressed as dimensionless constant separation factor, R_L , which is as follow:

$$R_L = \frac{1}{1 + K_L C_0} \quad (4)$$

where C_0 is the initial concentration and K_L is the Langmuir isotherm constant. The R_L values reflect the property of adsorption; $R_L > 1$ is unfavorable, $R_L = 1$ is linear, $0 < R_L < 1$: favorable and $R_L = 0$ is irreversible. In Figure 10, R_L versus C_0 has been plotted for both NaY and MY. It can be seen the values of R_L in whole region of initial concentrations are in the range between 0 to 1 for both NaY and MY which shows the adsorption is a favorable process [27,28]. In addition, it can be seen that by increasing the initial concentration, the adsorption are more favorable.

The K_F of Freundlich model which is related to adsorption capacity is relatively low for both adsorbents but the value for hierarchical MY indicates noticeable improvement and easier uptake of MB in comparison with microporous NaY zeolite (Table 3). Also, from the Freundlich, the values of $1/n$ 0.16 for NaY and 0.22 for

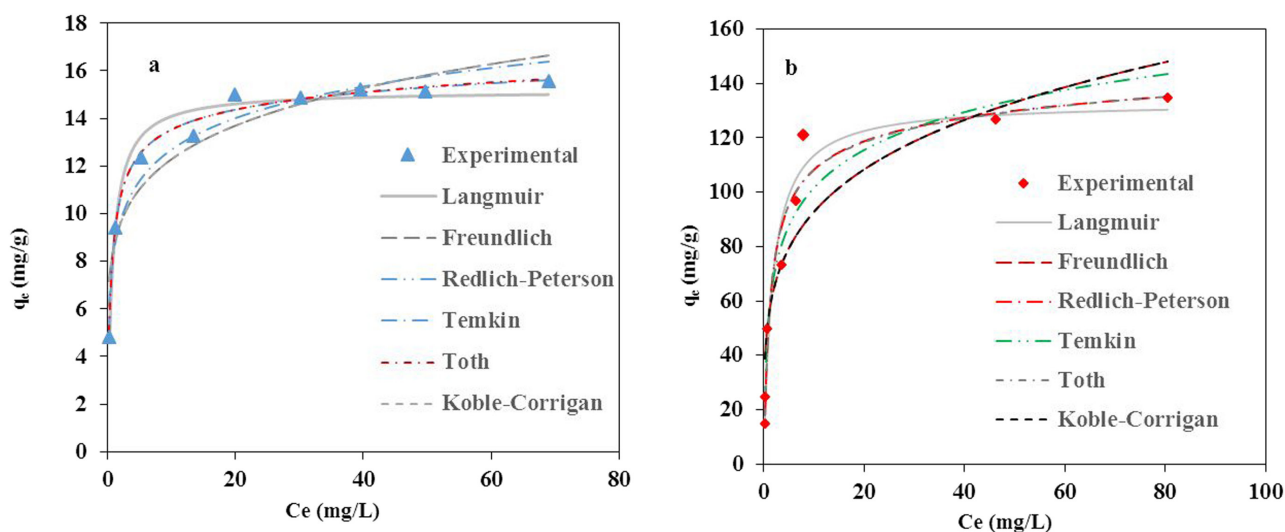


Figure 9: Equilibrium adsorption isotherms of methylene blue on (a) microporous NaY and (b) hierarchical MY.

Table 3: Isotherms parameters values for MB adsorption on microporous NaY and hierarchical MY.

Isotherm	Parameters	Values	
		NaY	MY
Langmuir	q_m (mg/g)	15.17	133.1
	K_L	1.3	0.58
	R^2	0.97	0.95
Freundlich	K_F	8.5	55.3
	n	6.3	4.46
	R^2	0.88	0.83
Redlich-peterson	A	26.7	113.4
	B	2.11	1.1
	g	0.95	0.94
	R^2	0.98	0.95
Temkin	A	8.26	55.5
	B	1.92	20.1
	R^2	0.94	0.94
Koble- Corrigan	A	2.87	13.27
	B	5.67	42.1
	n	0.16	0.22
	R^2	0.86	0.80
Toth	k_t	12.38	99.5
	a_t	0.47	0.92
	t	1.06	1.07
	R^2	0.98	0.95

MY have achieved which are located in the range of $0.1 < 1/n < 1$, indicative of a higher adsorbability of MB for both adsorbents [26]. As shown in Table 3, the Redlich-Peterson g parameter is almost 0.95 for both adsorbents which are near the value of 1 and implies that this isotherm is approaching Langmuir isotherm [26]. The Temkin parameters A and B were also listed in Table 3. From microporous NaY to hierarchical MY, the values of A and

Table 4: Comparison between maximum adsorption capacities (q_m) of various adsorbents in removal of MB.

Adsorbent	q_m (mg g ⁻¹)	Reference
Luffa cylindrical fibers	47.0	[27]
NaA _{mw} ¹	64.8	[28]
Alkaline-treated clinoptilolite	47.3	[29]
Au-NP-AC ²	104–185	[30]
PDA microspheres ³	90.7	[31]
Palm kernel fiber	95.4	[32]
Kaolin	45	[23]
Commercial zeolite	22	[23]
crosslinked chitosan/bentonite composite	95.24	[33]
ZnS:Cu-NP-AC ⁴	106.9	[34]
Fe3O4 NPs	89.2–91.9	[35]
Polyoxometalate	140.84	[36]
Leaves of Solanum tuberosum	52.6	[37]
Fe/SCD-LDH ⁵	80–100	[38]
hierarchical zeolite Y (MY)	133.1	This work

¹ microwave rapid synthesized NaA zeolite

² gold nanoparticles loaded on activated carbon

³ Polydopamine

⁴ ZnS:Cu nanoparticles loaded on activated carbon

⁵ magnetic Fe3O4@sulfonated β -cyclodextrin intercalated LDH

B became larger. This issue also confirms the improved characteristic of the hierarchical MY zeolite [26].

3.2.3 Kinetic studies

The kinetic studies are important in order to the industrialization of the adsorption process. The experimental data of kinetic was plotted in Figure 11. The Pseudo- first and second kinetic models, Eq. 2

and Eq. 3, were used for nonlinear curve fitting. Some publications evaluated the linear and non-linear methods for this purpose and concluded the non-linear methods may be more precise to attain the desired parameters of kinetic [39].

The values of parameters for each model has been inserted in Table 5. The correlation coefficient of Pseudo-second order for both microporous NaY and hierarchical MY are higher than their values of Pseudo-first order model. Therefore the adsorption kinetic obey Pseudo-second-order model. Several similar results were reported for the adsorption of MB on different adsorbents [24,27,40,41]. In addition to data which are achieved by isotherms studies of NaY and MY, the kinetic achievements

also proved that the mechanism of adsorption process has not altered during the modification process and obeys a similar procedure for both adsorbents.

3.2.4 Regenerated adsorbents performance

In order to assess the reusability of the adsorbent and investigation the performance of the modified hierarchical zeolite in successive adsorption process, the MY zeolite was recovered by calcination of MB in a microwave furnace at 500°C for 3 h. The removal efficiency versus the frequency of recycling has been plotted in Figure 12. It is seen that after four successive utilization of MY, a slight deterioration in the adsorption performance has occurred. The aggregation and cohesion of the adsorbent after several utilization of adsorbent can lead to reduction in surface area of adsorbent which resulted in decrease in the MB removal after several recovery processes [28].

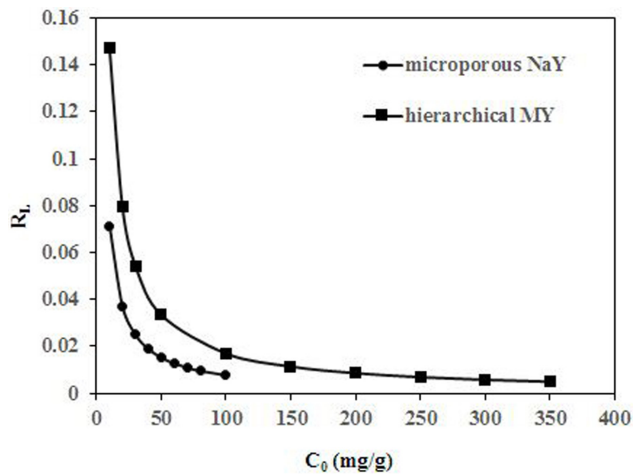


Figure 10: The Langmuir separation factor (R_L) for microporous NaY and hierarchical MY.

Table 5: Pseudo-first-order and Pseudo-second-order parameters for the adsorption of MB on NaY and MY.

Kinetic model	Parameters	Values	
		NaY	MY
Pseudo first order	q_e	19.01	46.3
	k_1	0.512	0.75
	R^2	0.912	0.95
Pseudo second order	q_e	20.13	48.08
	k_2	0.04	0.03
	R^2	0.97	0.98

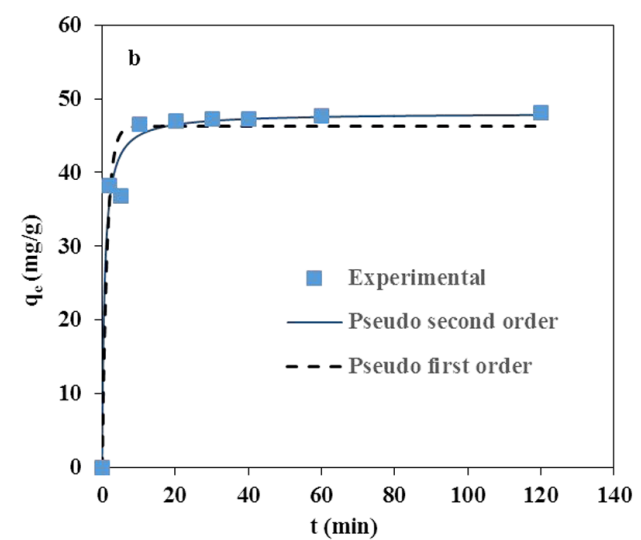
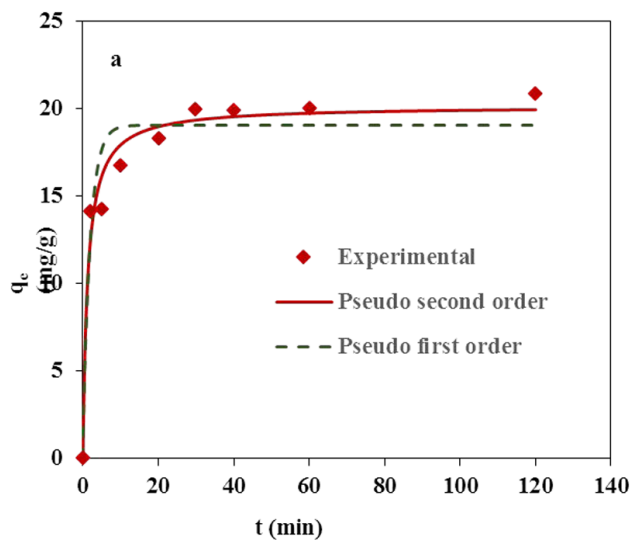


Figure 11: Pseudo-first order and pseudo-second-order kinetic models for (a) microporous NaY and (b) hierarchical MY.

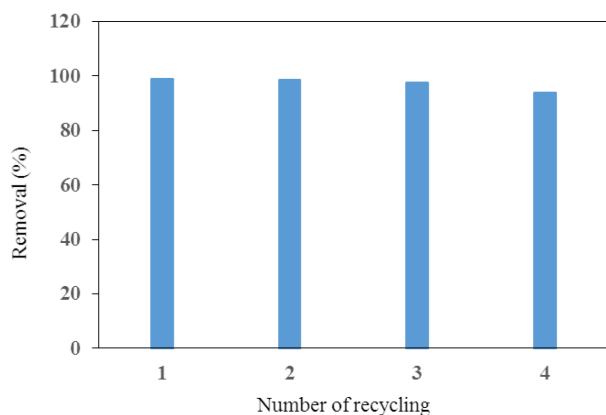


Figure 12: Plot of the reusability test adsorption of MB removal onto hierarchical MY.

4 Conclusions

In this study, a zeolite NaY with a low ratio of Si/Al = 2 was synthesized by silica extracted from rice husk ash. It is higher aluminum content made it a hydrophilic zeolite with a more negative charge which is favorable for the removal of cationic methylene blue dye from the water. After modification of the proposed zeolite to hierarchical one, MY, by a “destructive-constructive” method, the Si/Al ratio was maintained and some mesopores were inserted in the zeolite structure. The presence of these mesopores caused a synergistic effect in removal of methylene blue. The proposed MY possessed remarkable adsorption capacity of 133.1 mg g⁻¹ in comparison with the parent NaY zeolite (15.2 mg g⁻¹) in the removal of the methylene blue dye.

Acknowledgment: The authors thank the University of Mazandaran for financial support.

References

- [1] Visa M., Synthesis and characterization of new zeolite materials obtained from fly ash for heavy metals removal in advanced wastewater treatment. *Powder Technol.*, 2016, 294, 338-347.
- [2] Ghaedi M., Heidarpour S., Nasiri S., Sahraie R., Comparison of silver and palladium nanoparticles loaded on activated carbon for efficient removal of Methylene blue: Kinetic and isotherm study of removal process. *Powder Technol.*, 2012, 228, 18-25.
- [3] Shahryari Z., Goharrizi A.S., Azadi M., Experimental study of methylene blue adsorption from aqueous solutions onto carbon nano tubes. *Int. J. Water Resour. Environ. Eng.*, 2010, 2, 16-28.
- [4] Rafatullah M., Sulaiman O., Hashim R., Ahmad A., Adsorption of methylene blue on low-cost adsorbents: A review. *J. Hazard. Mater.*, 2010, 177, 70-80.
- [5] Jin X., Jiang M., Shan X., Pei Z., Chen Z., Adsorption of methylene blue and orange II onto unmodified and surfactant-modified zeolite. *J. Colloid Interface Sci.*, 2008, 328, 243-247.
- [6] J. Čejka J., Mintova S., Perspectives of Micro/Mesoporous Composites in Catalysis. *Catal. Rev. Sci. Eng.*, 2007, 49, 457-509.
- [7] Ramezani H., Azizi S.N., Hosseini S.R., NaY zeolite as a platform for preparation of Ag nanoparticles arrays in order to construction of H₂O₂ sensor. *Sensor. Actuat. B-Chem.*, 2017, 248, 571-579.
- [8] Corma A., From Microporous to Mesoporous Molecular Sieve Materials and Their Use in Catalysis. *Chem. Rev.*, 1997, 97, 2373-2419.
- [9] Kulprathipanja S. (Ed.), Zeolites in Industrial Separation and Catalysis. Wiley-VCH, 2010.
- [10] Sachse A., Wuttke C., Díaz U., de Souza M.O., Mesoporous Y zeolite through ionic liquid based surfactant templating. *Micropor. Mesopor. Mat.*, 2015, 217, 81-86.
- [11] Yan Y., Guo X., Zhang Y., Tang Y., Future of nano-/hierarchical zeolites in catalysis: gaseous phase or liquid phase system. *Catal. Sci. Technol.*, 2015, 5, 772-785.
- [12] Taylor P., Van Donk S., Janssen A.H., Bitter J.H., De Jong K.P., Generation, Characterization, and Impact of Mesopores in Zeolite Catalysts. *Catal. Rev. Sci. Eng.*, 2003, 45, 297-319.
- [13] Zhang K., Ostraat M.L., Innovations in hierarchical zeolite synthesis. *Catal. Today*, 2016, 264, 3-15.
- [14] Wang S., Dou T., Li Y., Zhang Y., X Li., Yan Z., A novel method for the preparation of MOR/MCM-41 composite molecular sieve. *Catal. Commun.*, 2005, 6, 87-91.
- [15] García-Martínez J., Li K., Krishnaiah G., A mesostructured Y zeolite as a superior FCC catalyst – from lab to refinery. *Chem. Commun.*, 2012, 48, 11841-11843.
- [16] Shultz J.L., A Simple Method for Production of Pure Silica from Rice Hull Ash. *Bioresource Technol.*, 2000, 73, 257-262.
- [17] Chal R., Cacciaguerra T., Donk V., Ge C., Pseudomorphic synthesis of mesoporous zeolite Y crystals. *Chem. Commun.*, 2010, 46, 7840-7842.
- [18] García-Martínez J., Johnson M., Valla J., Li K., Ying J.Y., Mesostructured zeolite Y-high hydrothermal stability and superior FCC catalytic performance. *Catal. Sci. Technol.*, 2012, 2, 987-994.
- [19] Shahid A., Lopez-Orozco S., Marthala V.R., Hartmann M., Schwieger W., Direct oxidation of benzene to phenol over hierarchical ZSM-5 zeolites prepared by sequential post synthesis modification. *Micropor. Mesopor. Mat.*, 2017, 237, 151-159.
- [20] Robson H., Verified synthesis of zeolitic materials (2 ed.). Elsevier, 2001.

- [21] Lowell S., Shields J., Thomas M., Thommes M., Characterization of porous solids and powders: surface area, pore size and density. Kluwer Academic Publishers, 2004.
- [22] Yang R.T., Adsorbents: fundamentals and applications. John Wiley & Sons, 2003.
- [23] Rida K., Bouraoui S., Hadnine S., Adsorption of methylene blue from aqueous solution by kaolin and zeolite. Appl. Clay Sci., 2013, 83-84, 99-105.
- [24] Hameed B.H., Removal of cationic dye from aqueous solution using jackfruit peel as non-conventional low-cost adsorbent. J. Hazard. Mater., 2009, 162, 344-350.
- [25] Gimbert F., Morin-Crini N., Renault F., Badot P.M., Crini G., Adsorption isotherm models for dye removal by cationized starch-based material in a single component system: Error analysis. J. Hazard. Mater., 2008, 157, 34-46.
- [26] Han R., Zhang J., Han P., Wang Y., Zhao Z., Tang M., Study of equilibrium, kinetic and thermodynamic parameters about methylene blue adsorption onto natural zeolite. Chem. Eng. J., 2009, 145, 496-504.
- [27] Demir H., Top A., Balköse D., Ülkü S., Dye adsorption behavior of *Luffa cylindrica* fibers. J. Hazard. Mater., 2008, 153, 389-394.
- [28] Sapawe N., Jalil A.A., Triwahyono S., Shah M.I.A., Jusoh R., Salleh N.F.M., et al., Cost-effective microwave rapid synthesis of zeolite NaA for removal of methylene blue. Chem. Eng. J., 2013, 229, 388-398.
- [29] Akgül M., Karabakan A., Microporous and Mesoporous Materials Promoted dye adsorption performance over desilicated natural zeolite. Micropor. Mesopor. Mat., 2011, 145, 157-164.
- [30] Roosta M., Ghaedi M., Daneshfar A., Sahraei R., Asghari A., Optimization of the ultrasonic assisted removal of methylene blue by gold nanoparticles loaded on activated carbon using experimental design methodology. Ultrason. Sonochem., 2014, 21, 242-252.
- [31] Fu J., Chen Z., Wang M., Liu S., Zhang J., Zhang J., et al., Adsorption of methylene blue by a high-efficiency adsorbent (polydopamine microspheres): Kinetics, isotherm, thermodynamics and mechanism analysis. Chem. Eng. J., 2015, 259, 53-61.
- [32] El-Sayed G.O., Removal of methylene blue and crystal violet from aqueous solutions by palm kernel fiber. Desalination, 2011, 272, 225-232.
- [33] Bulut Y., Karaer H., Adsorption of Methylene Blue from Aqueous Solution by Crosslinked Chitosan/Bentonite Composite. J. Dispers. Sci. Technol., 2015, 36, 61-67.
- [34] Asfaram A., Ghaedi M., Hajati S., Rezaeinejad M., Goudarzi A., Purkait M.K., Rapid removal of Auramine-O and Methylene blue by ZnS: Cu nanoparticles loaded on activated carbon: A response surface methodology approach. J. Taiwan Inst. Chem. Eng., 2015, 53, 80-91.
- [35] Ghaedi M., Hajjati S., Mahmudi Z., Tyagi I., Agarwal S., Maity A., et al., Modeling of competitive ultrasonic assisted removal of the dyes - Methylene blue and Safranin-O using Fe₃O₄ nanoparticles. Chem. Eng. J., 2015, 268, 28-37.
- [36] Rabbani M., Seghatoleslami Z.S., Rahimi R., Selective adsorption of organic dye methylene blue by Cs₄H₂PMo₁₁FeO₄₀•6H₂O in presence of methyl orange and Rhodamine-B. J. Mol. Struct., 2017, 1146, 113-118.
- [37] Gupta N., Kushwaha A.K., Chattopadhyaya M.C., Application of potato (*Solanum tuberosum*) plant wastes for the removal of methylene blue and malachite green dye from aqueous solution. Arab. J. Chem., 2016, 9, S707-S716.
- [38] Hu W., Wu X., Jiao F., Yang W., Zhou Y., Preparation and characterization of magnetic Fe₃O₄@sulfonated β-cyclodextrin intercalated layered double hydroxides for methylene blue removal. Desalin. Water Treat., 2016, 57, 25830-25841.
- [39] Raghunadh Acharyulu S., Gomathi T., Sudha P.N., Physico-chemical characterization of cross linked chitosan-polyacrylonitrile polymer blends. Der Pharm. Lett., 2013, 5, 354-363.
- [40] Ponnusami V., Vikram S., Srivastava S.N., Guava (*Psidium guajava*) leaf powder: Novel adsorbent for removal of methylene blue from aqueous solutions. J. Hazard. Mater., 2008, 152, 276-286.
- [41] Özer A., Dursun G., Removal of methylene blue from aqueous solution by dehydrated wheat bran carbon. J. Hazard. Mater., 2007, 146, 262-269.